Egyptian Journal of Physics

https://ejphysics.journals.ekb.eg/

Characterizing the Physical Properties of Polyvinylidene Fluoride/ Cellulose Nanocrystal Nanocomposite Fibers for Smart Textiles Applications.

Afaf M. Ali

Physics Department, Faculty of Science, Mansoura University, Egypt

Corresponding author email address: afafmaweed@gmail.com

Abstract

Understanding the polyvinylidene fluoride (PVDF) monofilament biocompatibility, biodegradation resistance and its ease handling get a great attention nowadays. In this study, Polyvinylidene difluoride (PVDF) was used as the matrix, whereas cellulose nanocrystal (CNC) were utilized as a nanofiller to produce nanocomposite fibres (PVDF/CNC). The concentrations of nanofillers (CNC) were 0, 1wt.%, 2 wt.%, and 3 wt.%. The under study filaments were subjected to a specific treatment for enhanced performance. Structural and mechanical properties were determined using DSC, XRD, optical polarizing microscopy. The melting temperature, glass transition temperature, crystalinity, the birefringence and the different molecular orientations were measured for the samples under study. Results confirmed that the interaction of PVDF and CNC was strong and led to enhance the different physical properties of the used nanocomposite fibres in this study. This finding might be considered a result of nanocrystal accumulation.

Keywords: PVDF, X-ray Diffraction, Differential Scanning Calorimetry, crystallinity, Birefringence, and orientation.

Introduction

Nanocomposites can be used in various applications of smart textile such as defense shield, sensors, self-cleaning, anti-bacterial, moisture management, fire protection, energy harvesting and actuators [1-11]. A smart textile can detect changes in the surroundings and react by changing one or more of its restrictions to

*Corresponding author: Afaf M. Ali, E-mail: afafmaweed@gmail.com.
Received: 19/12/2023; Accepted: 16/01/2024
DOI: 10.21608/EJPHYSICS.2024.255719.1096

implement a function [5]. A main form of nanocomposites used in smart textile applications is the fiber form. The fiber reveals a nano-composite constitution itself. Using this form, different functionalities can be merged into the fiber [4].

Nanocomposite substances are fundamentally harmonious in nature where two phases. The two phases are the reinforcement and the matrix that combined to complement one another. To provide a exclusive chance of creating essentially smart structures [12]. Therefore, to synthesize a nanocomposites fiber utilized in smart textile applications, Polyvinylidene difluoride (PVDF) selected as the matrix, whereas varying amounts of cellulose nanocrystal (CNC) were incorporated as a nanofiller to fine-tune structural and physical properties.

Polyvinylidene difluoride (PVDF) is an extremely nonreactive thermoplastic polymer. which has elicited curiosity due to its elasticity and exclusive electroactive properties. it can be used in different wearable devices or smart textiles [13-16]. PVDF is a semicrystalline polymer that has high mechanical strength, good chemical resistance, high thermal constancy and exceptional chemical resistance to corrosive chemicals [17]. The PVDF molecule has three unique structural phases (i.e. α, β and γ) depending on the conformation of chains [18].

During this study, a new nanofiller known as cellulose nanocrystal (CNC) was used. One of its important features is the presence of many functional groups on its surface. These functional groups are located on the surface with high surface area [19]. This property indicates that CNC shows potential for different applications because of enhanced dispersibility. It can also asset the inter-molecular interface with formed material matrix [20,21]. This vital advantage of PVDF/CNC nanocomposites material enhances the mechanical.

In this study PVDF/CNC nanocomposite fibres were used. Different physical properties such as crystalinity, birefringence, different molecular orientation for PVDF, PVDF/CNC1, PVDF/CNC2 and PVDF/CNC3 were determined at different draw ratios (DR) during the cold drawing process.

2- Structural parameters measurement of PVDF/CNCs composite fibers using different techniques:

The PVDF/CNC nanocomposite fibers were obtained using spinning unit depending on the dry-jet wet spun process. To improve the different industrial applications of the nanocomposite fibers it should be exposed to an exterior effect such as the mechanical cold drawing process. The different structural and physical properties

should be evaluated after the external effect application. The degree of crystallinity of treated PVDF/CNC nanocomposite could be measured using the following techniques XRD and DSC.

a) Differential scanning calorimetry:

The crystallinity and some other physical parameters as temperature of melting and temperature of glass transition can be evaluated using the DSC technique. A Perkin- Elmer Diamond -7 DSC device was used to determine the DSC thermograms of different PVDF samples[20]. The tested sample mass was 10 mg. The recorded thermograms were taken in temperature range (100 ^{o}C - 250 ^{o}C). The heating rate was 10 °C/min. The crystallinity (χ_c) of PVDF different samples can be measured. Using the measured fusion enthalpy ΔH_f and the theoretical heat fusion at complete crystallization ΔH_f^0 using the following equation [22]:

$$\chi_c = \frac{\Delta H_f}{\Delta H_f^0} \text{ x } 100 \qquad (1)$$

Where the heat of fusion for 100% crystalline of PVDF sample ($\Delta H_f^0 = 104.7\, J/g$)

b) Wide- angle X-Ray scattering (WAXS) technique:

The micro-structural properties of the under study samples of PVDF can be achieved by using X-ray diffractometer. Brucke-D8 was the model of the diffractometer used in this study. The wavelength of the Nickel-filteredline was (λ = 0.154 nm). It conducted at 45 kV, 66 mA. The radiation has been monochromatized with the aid of a monochromator beam made from graphite. The diffractograms for CNC nanoparticles and the different treated PVDF samples were recorded digitally in a range of 2θ from 5˚ to 50˚. The weight fraction crystallinity χ_c for the samples of PVDF measured using the following equation [21].

$$\chi = \frac{I_{cry}}{I_{cry}+I_{amp}} \qquad (2)$$

Where I_{cry} the area enclosed under the crystalline peak and I_{amp} the area enclosed under the amorphous peaks.

c) Geometrical parameters measurement of PVDF/CNCs composite fibers:

The geometrical parameters of the tested samples can be measured using a set-up of laser diffraction technique [21,23]. The fiber diameter (d) of tested samples can be measured using equation(3)

$$d = \frac{2\lambda l}{a} \qquad (3)$$

where *l* is the distance between screen and the fiber. The distance between the centers of the first maximum and the first minimum was (*a)*. The wavelength of the He–Ne laser was (λ =632.8 nm).

d) Birefringence determination of PVDF/CNCs composite fibers

The birefrigence (double refraction) can be pondered as an guide of the optical parameters and the molecular orientations of the different samples under consideration. An optical polarized light microscope was used to measure the birefringence of the different PVDF samples. The birefringence can be measured by means of Michel-Levy chart and equation(4) [23].

$$\Delta n = \frac{\boldsymbol{Phase\ Retardation}}{\boldsymbol{1000d}} \quad (4)$$

A certain adhesion material was used to fix the sample on the glass slide. Then, the slide transferred to the stage of the used microscope. The microscope accommodated until obtaining the maximum interference colors. In the Michel-Levy chart, a diagonal line will be chosen with slope equal to $(\frac{1}{\Delta n})$.

e) Characterization

The tensile properties calculated using a suitable single filament tensile tester. Its gauge length was 25 mm. At least 10 samples of the filaments were tested for each case (treated sample).

3. Results and Discussion

Nowadays, nanofillers has drawn a substantial consideration in diverse fields of nanocomposite such as GO and CNC. Because of their exclusive physical features. One of the most important physical properties is their large surface area. The surface functional group empowers them to interact powerfully with the whole matrix of the polymer[8,9]. In this work, CNC nanofillers fused in PVDF polymer with concentration ranged from (1-3 wt%) was used.

The mechanical properties were calculated by means of a suitable tensile tester. Its gauge length was 25mm. The stress-strain curves for different samples were calculated. Figure 1 shows the stress-strain curves of drawn treated samples of PVDF, PVDF/CNC_1 , PVDF/CNC_2 and PVDF/CNC_3. The mechanical properties such as the tensile-strength and the tensile-modulus were calculated for the samples under consideration. Table (1) illustrate the calculated tensile-strength and tensile-modulus for PVDF, PVDF/CNC_1 , PVDF/CNC_2 and PVDF/CNC_3. It is clear that, the calculated tensile strength and tensile modulus increase by increasing the CNCs addition. However, for PVDF/CNC_3 the measured modulus were less than the reference sample. This decrease can be considered as a result of CNC nanoparticles sever accumulation. This behaviour detected formerly for diverse polymer-based nanocomposites at high concentration of the nanofillers independent on the nanofiller kind [25-27].

Table 1. The calculated tensile strength and tensile modulus of the samples under consideration.

Sample	**Tensile Strength (Mpa)**	**Tensile Modulus (Gpa)**
PVDF	245.5	3.68
PVDF/CNC_1	307.4	4.12
PVDF/CNC_2	335.6	4.65
PVDF/CNC_3	232.4	3.76

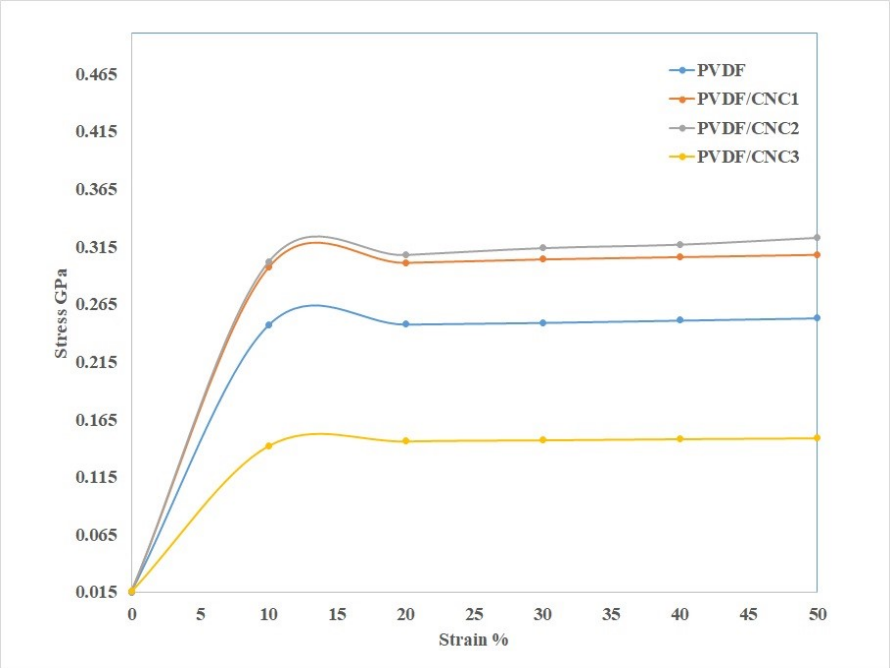

Fig. 1. Illustrate the stress-strain curves of drawn treated samples of PVDF,PVDF/CNC_1 , PVDF/CNC_2 and PVDF/CNC_3.

DSC technique was used to study the interaction between CNC and PVDF throw measuring the different thermal properties as the glass transition temperature and the melting temperature. Figure 2 gives the calculated glass transition temperature at different draw ratios for PVDF, PVDF/CNC_1 , PVDF/CNC_2 and PVDF/CNC_3samples. It is clear that T_g increase by increasing the draw ratio and also with increasing the CNCs addition. Figure 3 gives the calculated melting temperatures at different draw ratios for PVDF, PVDF/CNC_1 , PVDF/CNC_2 and PVDF/CNC_3. Using equation (1) the Crystallinity was measured. Figure 4 shows the calculated crystallinity for PVDF, PVDF/CNC_1 , PVDF/CNC_2 and PVDF/CNC_3 at different draw ratios. The crystallinity increased with increasing the draw ratio for all the samples under investigation. But the measured crystallinity of PVDF/CNC_3 fiber are quite lower than the reference PVDF fiber at all DRs.

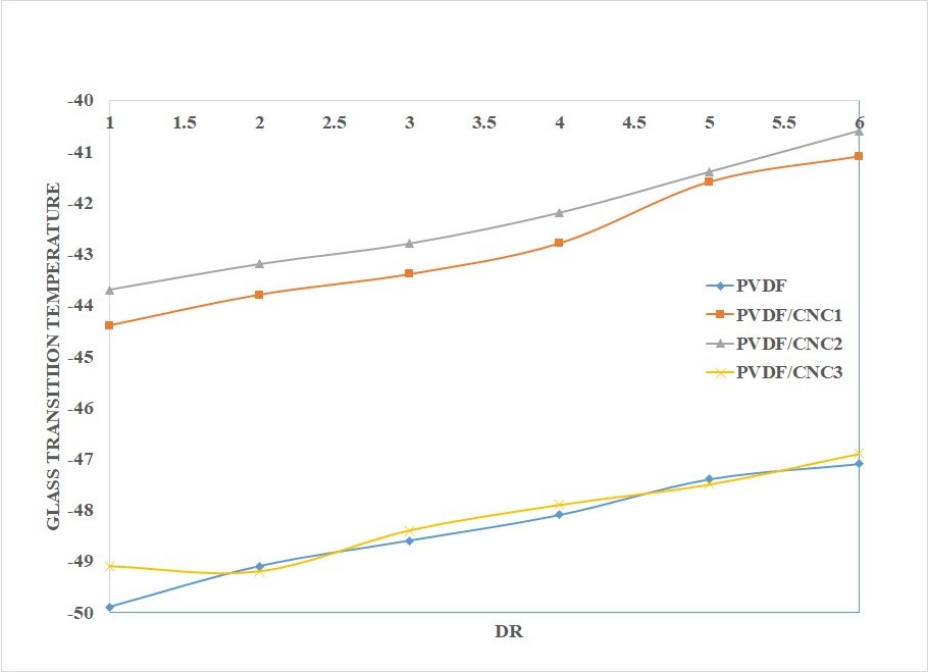

Fig. 2. The calculated glass transition temperature at different draw ratios for PVDF, PVDF/CNC_1 , PVDF/CNC_2 and PVDF/CNC_3samples.

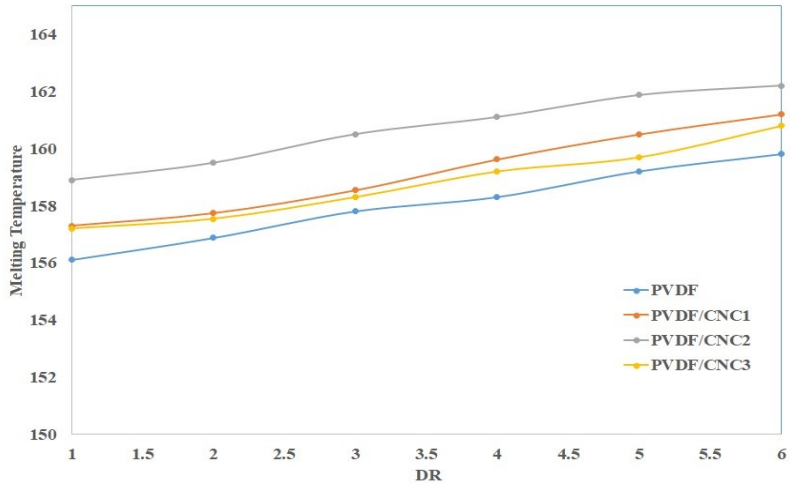

Fig. 3. The calculated melting temperatures at different draw ratios for PVDF, PVDF/CNC_1 , PVDF/CNC_2 and PVDF/CNC_3.

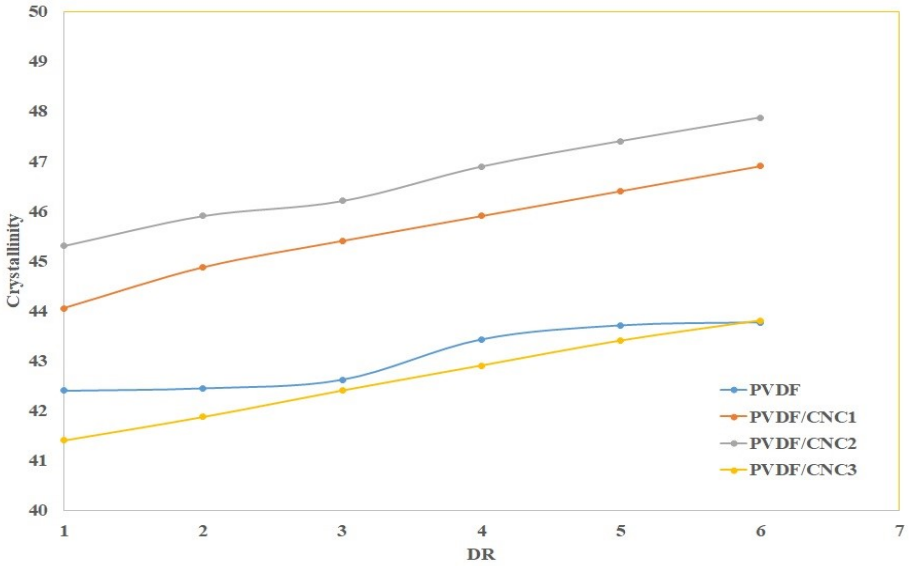

Fig. 4. The calculated crystallinity for PVDF, PVDF/CNC_1 , PVDF/CNC_2 and PVDF/CNC_3 at different draw ratios.

X- Ray diffraction technique can be used to study the interaction between PVDF and CNCs. Using equation (2), the crystallinity can be measured. Figure 5 shows the calculated crystallinity for PVDF, PVDF/CNC_1 , PVDF/CNC_2 and PVDF/CNC_3 at different draw ratios using XRD technique. It is clear that the crystallinity increased with increasing the draw ratio for all of the samples under investigation. Although, the measured crystalinity of PVDF/CNC_3 fiber are comparatively inferior to the recorded values for reference PVDF samples. The complete arrangement of the polymer chains due to strong-polar interaction among the matrix of PVDF and CNC nanofibers [9] causes the increase of crystallinity.

Using laser diffraction technique, the geometrical properties of the different samples was measured using equation (3). Figure 6 shows the calculated fiber radius of PVDF, PVDF/CNC_1 , PVDF/CNC_2 and PVDF/CNC_3 samples with the draw ratio. It is clear that as the draw ratio increase the fiber radius decrease gradually. All the samples started with fiber radius r≈ 30 μm and finally with fiber radius close to ≈ 15 μm.

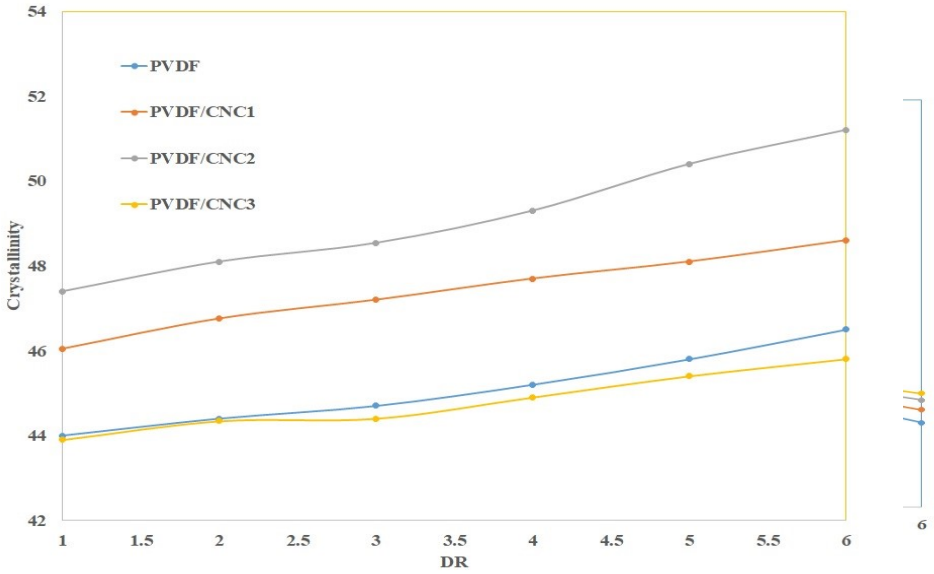

Fig. 5. The calculated crystallinity for PVDF, PVDF/CNC$_1$, PVDF/CNC$_2$ and PVDF/CNC$_3$ at different draw ratios using XRD technique.

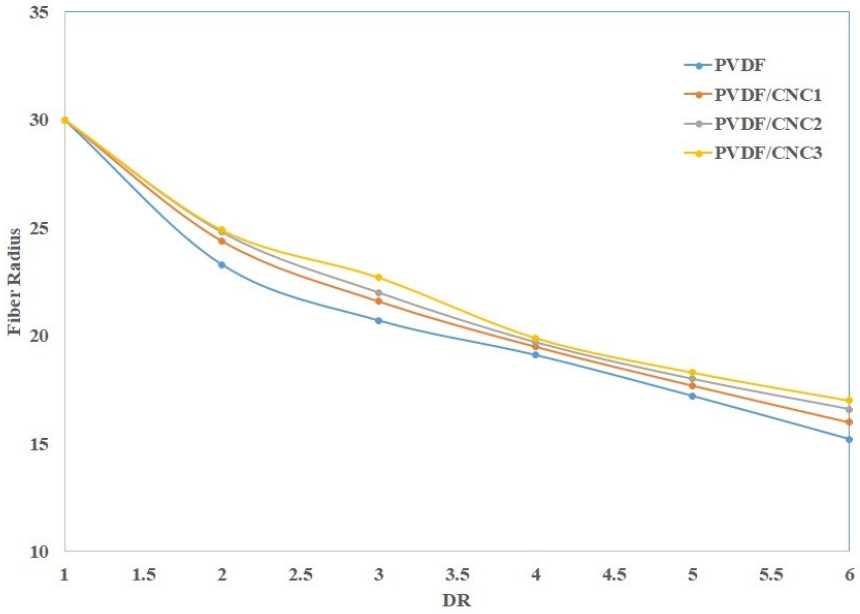

Fig. 6. The calculated fiber radius of PVDF, PVDF/CNC$_1$, PVDF/CNC$_2$ and PVDF/CNC$_3$ samples with the draw ratio.

To measure the birefringence of the different samples under consideration, the optical polarizing microscope with the aid of the measured fiber radius and equation (4) it can be measured. Figure 7 gives the variation of the calculated birefringence with the draw ratio for the samples PVDF, PVDF/CNC_1 , PVDF/CNC_2 and PVDF/CNC_3. It is clear that as the draw ratio increase the birefringence increase. The birefringence increased with increasing the draw ratio for all the samples under investigation. But the measured birefringence of PVDF/CNC_3 fiber are quite lower than the measured birefringence of the reference PVDF fiber at all DRs. The orientation of the fiber chain during the drawing process can be calculated using the Herman`s orientation function $f(\theta)$ with the aid of the following equation[21-23]:

$$f(\theta) = \frac{\Delta n}{\Delta n_{max}} \quad (5)$$

Where Δn the current birefringence, and Δn_{max} the maximum birefringence at fully orientation for PVDF $\Delta n_{max} = 0.043$. Figure 8 shows the variation of the calculated orientation function with the draw ratio for the samples PVDF, PVDF/CNC_1 , PVDF/CNC_2 and PVDF/CNC_3. The orientation function increased with increasing the draw ratio for all the samples under investigation. But the measured birefringence of PVDF/CNC_3 fiber are quite lower than the measured birefringence of the reference PVDF fiber at all DRs. The effect of the drawing process could be investigated from the orientation of the chains and the stuck angle. The stuck angle (θ) between the oriented chain and the fibre axis could be measured using the following equation[22].

$$\theta = \left[\frac{2}{3}(1 - f(\theta))\right]^{\frac{1}{2}} \quad (6)$$

The calculated stuck angles for PVDF, PVDF/CNC1, PVDF/CNC2 and PVDF/CNC3 samples are given in Table 2. As the DR increased, the chains got oriented, resulting in gradually decreasing stuck angle. The stuck angle of PVDF/CNC3 samples was higher than that of the control one.

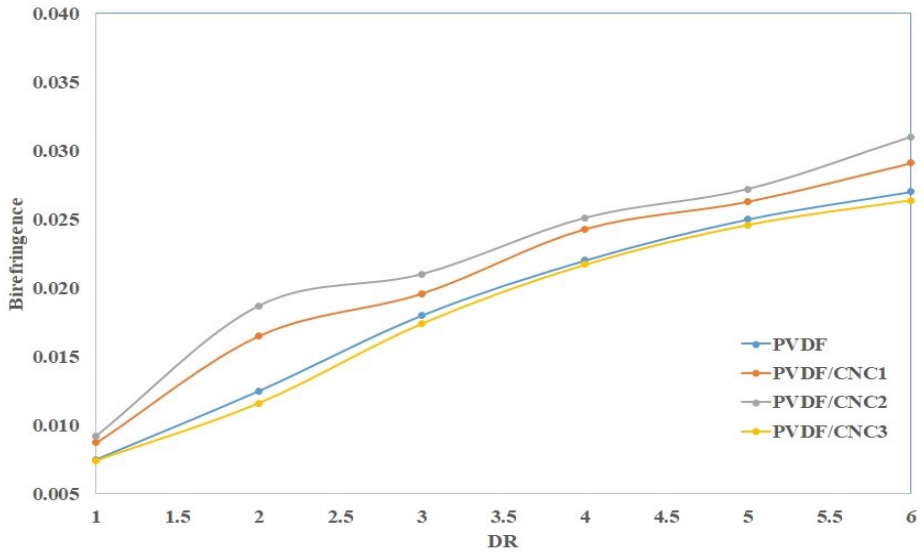

Fig. 7. The variation of the calculated birefringence with the draw ratio for the samples PVDF, PVDF/CNC$_1$, PVDF/CNC$_2$ and PVDF/CNC$_3$.

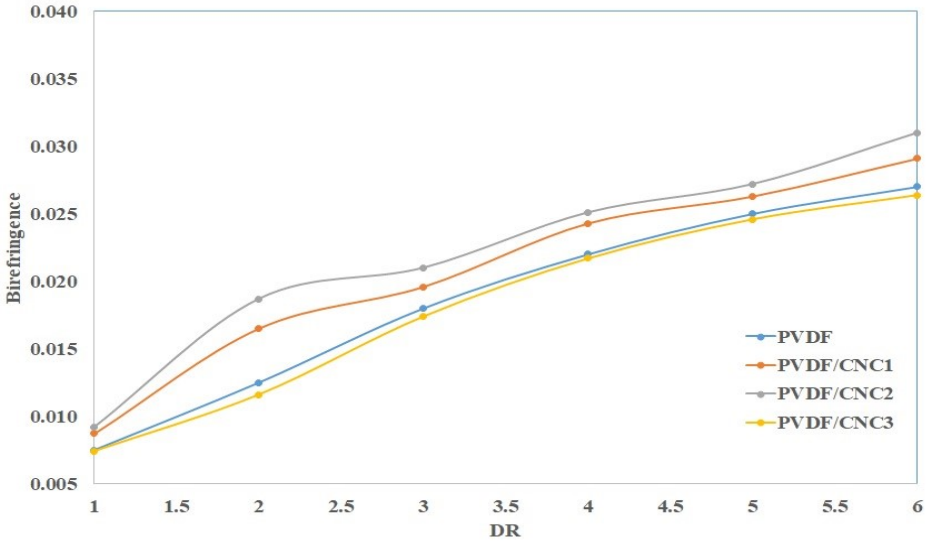

Fig. 8. The variation of the calculated orientation function with the draw ratio for the samples PVDF, PVDF/CNC$_1$, PVDF/CNC$_2$ and PVDF/CNC$_3$.

Table 2. The calculated stuck angle for the different samples under investigation at different draw ratio

	PVDF	PVDF/CNC1	PVDF/CNC2	PVDF/CNC3
Dr	**θ**	**θ**	**θ**	**θ**
1	47.89	46.82	46.32	47.98
2	43.44	39.86	37.86	44.25
3	38.5	37.04	35.48	39.05
4	34.79	32.58	31.79	35.08
5	31.88	30.59	29.66	32.28
6	29.88	27.66	25.55	30.48

The different molecular oerientations should be measured to charaterize the effect of the cold drawing process for the different samples under study using the following equations[22] :

$$f_2(\theta) = (3cos^2(\theta) - 1)/2$$

$$f_4(\theta) = (35cos^4(\theta) - 3cos^2(\theta) + 3)/8$$

$$f_6(\theta) = (231cos^6(\theta) - 15cos^4(\theta) + 150cos^2(\theta) - 5)/6$$

The different molecular orientations $f_2(\theta), f_4(\theta), f_6(\theta)$ were calculated for the different samples PVDF, PVDF/CNC_1 , PVDF/CNC_2 and PVDF/CNC_3 and illustrated in tables 3,4 and 5. It is clear that the different calculated molecular orientations for the samples under investigation icreased with increasing the draw ratio. While the measured molecular orientaions for PVDF/CNC_3 fiber are quite lower than the measured molecular orientaions for the reference PVDF fiber at all draw ratios. The measured physical parameters such as the birefringence and orientation function and the different molecular orientations confirm the great effect of the drawing process on enhancing the polymer chain orientations.

Table 3. The calculated molecular orientation $f_2(\theta)$ for the different samples under investigation at different draw ratio

	PVDF	PVDF/CNC1	PVDF/CNC2	PVDF/CNC3
Dr	**$f_2(\theta)$**	**$f_2(\theta)$**	**$f_2(\theta)$**	**$f_2(\theta)$**
1	0.175	0.20	0.21	0.17
2	0.29	0.38	0.43	0.27
3	0.42	0.46	0.49	0.41
4	0.51	0.57	0.58	0.50
5	0.58	0.61	0.60	0.57
6	0.63	0.68	0.72	0.61

Table 4. The calculated molecular orientation $f_4(\theta)$ for the different samples under investigation at different draw ratio

	PVDF	PVDF/CNC1	PVDF/CNC2	PVDF/CNC3
Dr	**$f_4(\theta)$**	**$f_4(\theta)$**	**$f_4(\theta)$**	**$f_4(\theta)$**
1	1.09	1.157	1.193	1.08
2	1.39	1.68	1.84	1.33
3	1.78	1.91	2.05	1.74
4	2.1	2.32	2.39	2.08
5	2.38	2.50	2.49	2.34
6	2.57	2.78	2.97	2.51

Table 5. The calculated molecular orientation $f_6(\theta)$ for the different samples under investigation at different draw ratio

	PVDF	PVDF/CNC1	PVDF/CNC2	PVDF/CNC3
Dr	**$f_6(\theta)$**	**$f_6(\theta)$**	**$f_6(\theta)$**	**$f_6(\theta)$**
1	13.43	14.26	14.72	13.30
2	17.29	20.94	23.05	16.51
3	22.32	24.02	25.83	21.82
4	26.67	29.49	30.44	26.31
5	30.31	32.01	31.86	29.76
6	32.89	35.87	38.59	32.16

4. Conclusion

Nanocomposite fibres displayed excellent mechanical properties. The tensile strength and modulus were measured at different concentrations of CNC. Mechanical properties improved as DR increased due to the increased chain orientations or extension in all fibres. The PVDF/CNC (2%) fibre showed the highest values of the tensile strength and modulus, but the mechanical properties of PVDF/CNC (3%) were less than those of reference or untreated PVDF. This decrease could be considered as a result of CNC nanoparticle overaccumulation as a result of discontinuity and heterogeneity in the microstructure. All samples had circular transverse sectional shapes. The high physical and mechanical properties of treated PVDF fibres permitted the production of textile sensors.

References

[1] Rajabzadeh, S., Maruyama, T., Sotani, T. and Matsuyama, H., *Sep. Purif. Technol*., **63,** 415 (2008).

[2] Yang, J., Zhao,W.M. and Wang, X.L., *Chem. J. Chin. Univ. Chin*., **29**, 1895 (2008).

[3] Sri, M., Sri, A., Syawaliah, M., Yanna S., Rosnelly, C. M, Muhammad, R. B., and Noor, M. I., *Polymers*, **14**, 186(2022) .

[4] Zhou, W., Jiang, X.Z., Wang, P. and Wang, H.T., *Fibers Polym*.,**14**, 100(2013).

[5] Maradini, G.S., Oliveira, M.P., Carreira, L.G., Guimarães, D., Profeti, D., Dias Júnior, A.F., Boschetti, W.T.N., Oliveira, B.F., Pereira, A.C. and Monteiro, S.N., *Polymers* , ***13,*** 1878(2021).

[6] Lee, J.E., Kim, Y.E., Lee, G.H., Kim, M.J., Eom, Y., Chae, H.G., *ACS Appl. Mater. Inter.*, **11,** 13665(2019).

[7] Liu, X., Ma, J., Wu, X.M., Lin, L.W., and Wang, X.H., *Chem. Eng. Nano*., **451**, 139077(2023).

[8] Lee, J.E., Kim, Y.E., Lee, G.H., Kim, M.J., Eom. Y., and Chae, H.G., *Compos Sci Technol*., **200**, 108452(2020).

[9] Zhang, Z., Wu, Q.L., Song, K.L., Ren, S.X., Lei, T.Z. and Zhang, Q.G., *ACS Sustain Chem Eng*., **3**, 574(2015).

[10] Zhang, Z., Wu, Q.L., Song, K.L., Lei, T.Z. and Wu, YQ*.,* "*Cellulose*, **22**, 2431(2015).

[11] Shah, M. and Bil, R., "Composites and Nanocomposites Functional Polymers", (2019) ISBN : 978-3-319-92067-2.

[12] Cheon, S., Kang, H., Kim, H., Son, Y., Lee, J.Y., Shin, H.J., Kim, S.W. and Cho, J.H., *Adv Funct Mater*., **28**, (2018)

[13] Lund, A., Rundqvist, K., Nilsson, E., Yu, L.¨ B, and Müller C., *npj Flexible Electronics*, **2**, 2(2018).

[14] Mokhtari, F., Spinks, G.M., Sayyar, S. and Foroughi, J., *Nanomaterials* , **11,** 2153(2021).

[15] Si, S.K., Paria, S., Karan, S.K., Ojha, S., Das, A.K., Maitra, A., Bera, A., Halder, L., De, A. and Khatua, B.B., *Nanoscale*, **12**, 7214 (2020).

[16] Kang, G. and Cao,Y.M., *J. Membr. Sci*., **463**, 145 (2014).

[17] Islam, A., Khan, A.N., Shakir, M.F. and Islam, K*., Mater. Res. Express*., **7,** 1(2020).

[18] Lee, J.E., Eom, Y., Shin, Y.E., Hwang, S.H., Ko, H.H. and Chae, H.G., *Compos Sci Technol*., **200**, 1016 (2020).

[19] Zhang, Z., Wu, Q.L., Song, K.L., Ren, S.X., Lei, TZ. *and* Zhang, Q.G., *Acs Sustain Chem Eng*., **3,** 574(2015).

[20] Zhang, Z., Wu, Q.L., Song, K.L., Lei, T.Z. and Wu, Y.Q., *Cellulose*, **22**, 2431(2015).

[21] Ali, A. M. and El-Dessouky, H. M., *Texti. Res*. **89**, 2(2019).

[22] Ali, A. M., *Micro. Res.and Techn*. **82**, 1922(2019).

[23] Ali, A. M. and Amin, A. H., *Micro. Res.& Techn*. **85**, 2659(2022).

[24] Forouzan, A., Yousefzadeh, M., Latifi, M. and Jose, R., "*Macromol Mater Eng.,* **306**, (2021).

[25] Conte, A. A., Shirvani, K., Hones, H., Wildgoose, A., Xue, Y., Najjar, R., Hu, X., Xue, W. and Beachley, V. Z., *Polymer*, **171**, 192(2019).

[26] Fu, Q. S., Zhang, W., Muhammad, I. P., Chen, X. D,. Zeng, Y., Wang, B.T., Zhang, S.Y., *Microporous Mesoporous Mater.,* **311**, 5436 (2021).

[27] Wu, L.K, Yuan, W.F., Nakamura, T., Atobe, S., Hu, N., Fukunaga, H., Chang, C., Zemba, Y., Li, Y., Watanabe, T., Liu, Y.L., Alamusi, Ning, H.M., Li, J.H., Cui, H. and Zhang, Y.J., *Adv Compos Mater*., **2**, 49(2017).

توصيف الخواص الفيزيائية لألياف (البولي فلوريد فينيلدين / ألياف السليلوز النانوية) لتطبيقات المنسوجات الذكية

عفاف على

قسم الفيزياء - كلية العلوم - جامعة المنصورة - مصر.

الخلاصة

إن فهم التوافق الحيوي للبولي فينيلدين ثنائي فلوريد (PVDF) ومقاومة التحلل الحيوي وسهولة التعامل معه يحظى باهتمام كبير في الوقت الحاضر. في هذه الدراسة، تم استخدام البولي فينيلدين ثنائي فلوريد (PVDF) كمادة أساسية، في حين تم استخدام بلورات السليلوز النانوية (CNC) كحشوة نانوية لإنتاج ألياف مركبة نانوية (PVDF/CNC). كانت تركيزات مواد الحشو النانوية 0 (CNC)، 1٪ ، 2٪ ، و 3٪. تم إخضاع الخيوط قيد الدراسة إلى معالجة محددة لتحسين الأداء. تم تحديد الخواص التركيبية والميكانيكية باستخدام DSC، XRD، والمجهر البصري الاستقطابي. تم قياس درجة حرارة الانصهار، درجة حرارة التزجيج، التبلور، الانكسار المزدوج، التوجهات الجزيئية المختلفة للعينات قيد الدراسة. أكدت النتائج أن تفاعل PVDF وCNC كان قوياً وأدى إلى تعزيز الخواص الفيزيائية المختلفة للألياف النانوية المركبة المستخدمة في هذه الدراسة. يمكن اعتبار هذا الاكتشاف نتيجة لتراكم البلورات النانوية.